Study the effect of applying benzimidazole-ethanol solution as a film-forming corrosion inhibitor on the surface of aluminium alloy 2024-t3

MUSSA, Magdi, LEWIS, Oliver, ZAHOOR, Deeba, TAKITA, Sarra and FARMILO, Nick <http://orcid.org/0000-0001-5311-590X>

chemistry proceedings

MDPI

Proceedings Paper

Study the Effect of Applying Benzimidazole-Ethanol Solution as a Film-Forming Corrosion Inhibitor on the Surface of Aluminum Alloy 2024-t3 †

Magdi Hassn Mussa [1,2,3,*], Sarra Takita [4], Farah Deeba Zahoor [4,5], Oliver Lewis [4] and Nicholas Farmilo [4,6]

[1] Mechanical and Energy Department, The Libyan Academy of Graduate study, Tripoli, Libya
[2] Mechanical Engineering Department, Sok Alkhamis Imsehel High Tec. Institute, Tripoli, Libya
[3] The Institute of Marine Engineering, Science and Technology, London, UK
[4] Materials and engineering Research institute MERI, Sheffield Hallam University, Howard Street, Sheffield, UK; Sarah.a.talita@gmail.com (S.T.); F.Zahoor@sheffield.ac.uk (D.F.); O.Lewis@shu.ac.uk (O.L.); nfarmilo@gmail.com (N.F.)
[5] Department of Chemistry, University of Sheffield, Sheffield, UK
[6] Tideswell Business Development Ltd., Ravensfield Sherwood Rd, Buxton, UK
* Correspondence: magdimosa1976@gmail.com; Tel.: +44-7404496955
† Presented at the 25th International Electronic Conference on Synthetic Organic Chemistry-Computational Chemistry at 15–30 November 2021.

Abstract: The Al-Cu-Mg light alloys storage such that their use for building structural, marine offshore, and aeroplane components with excellent strength/weight ratios would not be possible without adherent anti-corrosion preservation. Many techniques and strategies are still being used to treat the surface, such as cladding, anodising, and greasing. However, due to the cost, time consumed, and processing these techniques is considered complicated. Therefore, applying volatile organic inhibitors components are now being used effectively. Benzimidazole (BZI) and its derivatives are one of these film-forming chemicals used on copper and steel directly or as injectable combined with other carriers such as fatty acids or dissolvable hydrocarbons with high efficiency on corrosion protection. Therefore, this paper will investigate the enhancement of the corrosion protection afforded by direct spraying of BZI solution on the surface of aluminium alloy 2024-tThe corrosion protection performance results from the high electronegativity of BZI and as a film-forming inhibitor, which will be adsorbed on the metallic surface as it may emulate the active protection. The corrosion protection properties of the BZI film-forming coating were preliminary studied within 3.5% NaCl by using electrochemical impedance testing and simulations. The surface chemical adsorption confirmation was done by infrared spectroscopy (ATR-FTIR), supported by analysing the morphology of the surface before and after the immersion testing by using scanning electron microscopy (SEM) and real-image within one week of immersion. The Benzimidazole film-forming coating exhibited good anti-corrosion properties, providing an adherent protection film on AA 2024-t3 samples comparing to cladded bare AA2024-t3 with a cost-effective and easy applying process.

Keywords: volatile corrosion inhibitor; corrosion; adsorption; film-forming; AA 2023-t3

Citation: Mussa, M.H.; Takita, S.; Zahoor, F; Lewis, O; Farmilo, N. Study the Effect of Applying Benzimidazole-Ethanol Solution as a Film-Forming Corrosion Inhibitor on the Surface of Aluminum Alloy 2024-t3. *Chem. Proc.* **2021**, *3*, x. https://doi.org/10.3390/xxxxx

Published: date

1. Introduction

keeping and storing construction components on project sites need exceptional management and preservation to avoid damage and corrosion. Usually, the metallic part is more affected by the environment than other construction materials. Although it is still desirable due to its mechanical properties, such as steel, copper, and aluminium alloys, many preservation procedures could apply from the factory and on-site to reduce this effect from the surrounded environment [1].

Aluminium alloy 2xxx series is more desirable for aerospace and marine offshore construction projects due to its strength-weight ratio. Despite that, the aluminium alloys series is usually susceptible to corrosion more than pure aluminium due to micro galvanic effects and pitting corrosion caused by the presence of copper-containing intermetallic particles (IMPs), which disrupt the passivating aluminium oxide film on the alloy surface [2]. The different types of IMPs have their specific behaviour and electrochemical nature. These ionised phases include iron, manganese and silicon, which are considered impurities, and IMPs can create cathodic compounds consistent with aluminium itself.

The pitting corrosion mechanism generally consists of two stages which are initiation and propagation. In the presence of chloride ions on the oxide passive film on alloy, the weakest points on the passive oxide film will occur where some intermetallic particles (IMPs) are near the surface. Pitting corrosion will initiate and possibly grow depending on the local conditions, the alloy and electrolyte. In many cases, if the pit remains active, it will involve an internal micro galvanic cell. It will result in propagation-based upon physically separated aluminium oxidation and the oxygen or hydrogen reduction depending upon the electrode potential of metal and the solution. These equations can briefly give a describing mechanism of pitting corrosion on AA2024 alloy in aerated neutral and alkaline solution [3]

$$\boldsymbol{O_2 + 2H_2O + 4e^- \rightarrow 4OH^-} \quad (1)$$

$$\boldsymbol{O_2 + 4H^+ + 4e^- \rightarrow 2H_2O} \quad (2)$$

$$\boldsymbol{2H^+ + 2e^- \rightarrow H2} \quad (3)$$

$$\boldsymbol{H_2O + 2e^- \rightarrow 2OH^- + H_2} \quad (4)$$

$$\boldsymbol{Al^{3+} + 3H_2O \rightarrow Al(OH)_3 + 3H^+} \quad (5)$$

$$\boldsymbol{2Al \rightarrow 2Al^{3+} + 6e^-} \quad (6)$$

the creation of H^+ will occur as a result of the re-hydrolysis of aluminium ions Al^{3+} and this will lead to acidify the media around the pit and lowering the pH lower than 3 pH. Therefore, from equation 6, because of acidifying the solution inside the pit, the local environment will become more aggressive, causing Al dissolution. However, the process continues, hence causing the autocatalytic propagation of the pit. Figure 1, shows the schematic of the mechanism of pitting in the aluminium-copper based alloys.

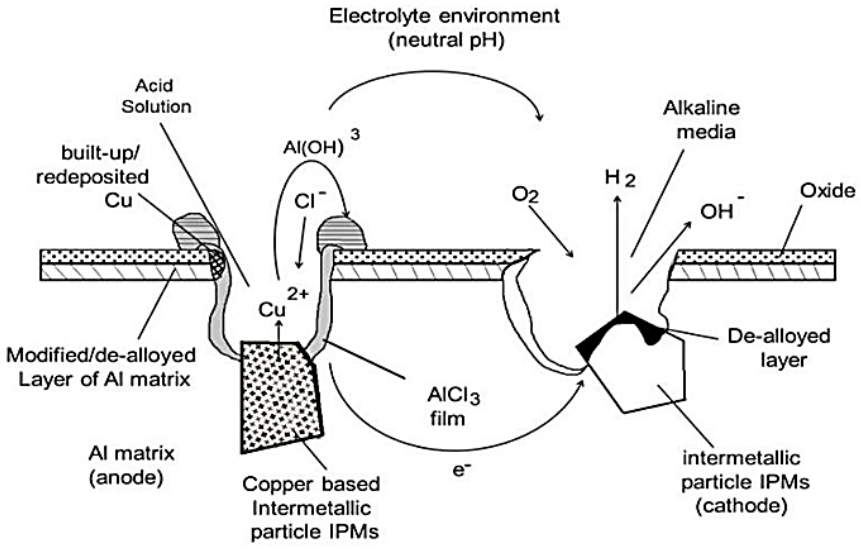

Figure Schematic mechanism of pitting corrosion on aluminium AA2024 [4].

The figure illustrates the common mechanism of pitting in AA2024-T3 alloy resulting from the presence of intermetallic particles, which cover about 3 to 4% of the overall surface area. A majority of these (approximately 60%) IPMs are (Al_2MgCu) S-phase- saturated sold solutions [5,6]. This S-phase is mainly responsible for the corrosion on this alloy as it

is more electrochemically active (anodic) than the alloy itself. The electrochemical dissolution of Al and Mg from the S-phase will start during the initial stages of the corrosion process leaving behind copper, which accumulates on the side of pits as a thin film due to the continuous dissolution of the remaining copper [2,3,6,7]. This thin film of copper around the pits is crucial in developing the localised and micro-galvanic corrosion, causing a growth in the cathodic area and increasing the anodic current density in the pit. Thus, suppressing S-phase de-alloying and deposited copper on AA2024 alloys will positively affect any localised corrosion inhibition strategy.

Many techniques for preservation, such as cladding with a thin film of pure aluminium or copper, improve its surface corrosion protection[8,9]. Alternatively, organic inhibitors that can either react with IPMs and S-phase will provide a robust inhibition process. [10,11].

Today, there is a wide range of volatile inhibitor formulations that may be used for corrosion protection of both ferrous or non-ferrous metals, such as benzimidazole, 2-benzimidazolethiol, and 2-mercaptobenzothiazole, these having been reported as effective inhibitors on copper, steel, zinc and their alloys [11]. As the Benzimidazole (BZI) is one of the imidazole derivatives that has been identified as low pH film-forming corrosion inhibitors with the structure of a heterocyclic aromatic organic compound, which could be used as both effective VCI or injectable inhibitor with other soluble carriers due to the chemical structure that contains both a benzene group. Also, the active group imidazole can be used in the oil and gas industry by using inhibitors injection pumps [12]. Generally, it was found that the BZI and its derivatives may be seen in this inhibitor molecule positioned in a parallel adsorption arrangement, and there was a close joining with the surface [13,14].In addition, BZI is available commercially as a raw material for many applications, the primary use being in pharmaceutical applications to use as a fungicide [15].

This paper will study the enhancement of corrosion protection that could be provided by spraying an ethanol solution of benzimidazole on aluminium alloys 2024-t3 in a standard 3.5% NaCl solution.

2. Experimental and Work Procedure

2.1. Substrate Preparation and Film Deposition

The commercially aluminium alloy AA2024-T3 Q-panels made with dimensions of (102 mm × 25 mm × 1.6 mm) were purchased from Q-Lab for use as test substrates [16]. First, the received Q-panels were washed with a commercial aluminium base surfactant cleaner and then rinsed with DI water; after that, rewashed with acetone to remove organic residues on the surface. Then spry the BZI solution, "which is pre-prepared from 1:3 v/v BZI and Ethanol" to the pre-cleaned aluminium alloy substrates over three passes. After that, the coated samples were left in the air for 10 min. The BZI treated samples were labelled as BZI-AA 2024, and the other nontreated was labelled as Bare-AA 2024.

2.2. Coating Testing and Characterisation

Electrochemical tests were performed on the coatings to assess their corrosion resistance. Tests were conducted by using a Princeton Applied Research PARSTAT The corrosion performance will be evaluated using potentiodynamic polarisation scans (PDPS), and electrochemical impedance spectroscopy (EIS) on The BZI coated and uncoated aluminium alloy samples. The tested area of 1.00 cm^2 in the centre of the samples in aerated 3.5% NaCl solution. The tests were carried at room temperature (20 °C +/- 2 °C). Prior to polarisation, the electrode potential was monitored for approximately 1 h in electrolyte solution until stability. The sample was polarised with PDPS at a scan rate of 1.667 mVs^{-1} from the initial potential of −250 mV vs OCP to +750 mV vs SCE. The electrochemical impedance measurements were recorded between 100 kHz to 10 MHz with a sinusoidal AC RMS value of 10 mV [17].

3. Results and Discussion

3.1. The Potentiodynamic Polarisation Scans (PDPS)

The corrosion and corrosion protection for the bare and treated BZI-AA2024 samples was investigated by potentiodynamic polarisation in the standard NaCl solution, as is shown in Figure The anodic and cathodic behaviour was measured between −250 mV and 750 mV against the tested sample's open circuit potential (OCP). As shown Figure 2, by using Tafel exploiting, the bare AA2024 sample has a corrosion current of 6.9×10^{-6}A/cm^2. The anodic branch of the uncoated sample shows the continuous active dissolution of the metal, while the cathodic branch exhibits diffusion control. The corrosion current density (I_{corr}) of the pre-treated benzimidazole sample BZI-AA2024 is about one order of magnitude lower than the untreated bare-AA2024 sample, with the result at about 5.1×10^{-7}A/cm^2.

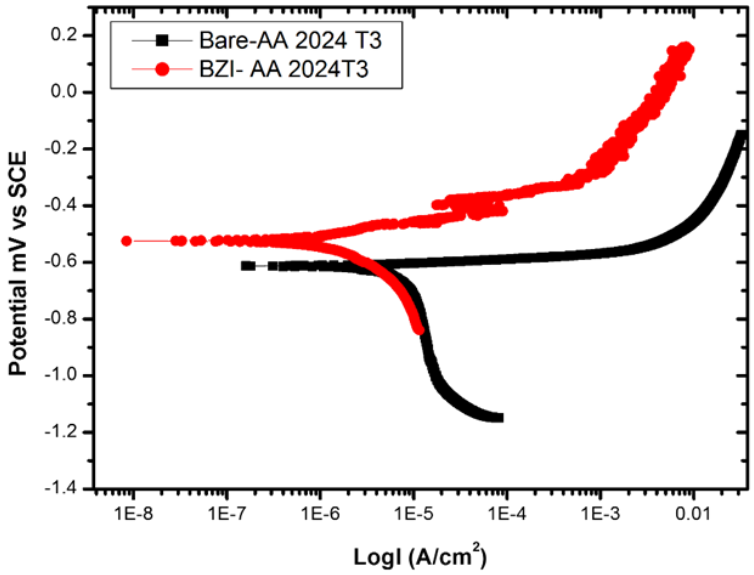

Figure 2. (PDPS) Polarization curves for the bare and BZI coated samples in 3.5% NaCl.

The corrosion potential of bare AA2024 was measured at -612 ± 2 mV (SCE), while the BZI-AA2024 was measured at -565 ± 2 mV (SCE) respectively. The cathodic branches showed different diffusion control on all treated samples. The pitting potential of BZI bare AA2024 was about −500 mV suggests that the pitting may here be commenced. The cathodic branch of the BZI treated sample was stabilised with one order of magnitude lower than the Bare.

Showed the summarised PDPS polarisation data:

Table PDPS polarisation data for both samples.

Sample	E_{corr}[mV] (Vs SCE)	I_{corr} [A/cm^2]	Average OCP mV vs. SCE
Bare-AA2024	-612 ± 2	6.9×10^{-6}	610
BZI-AA2024	-565 ± 2	5.1×10^{-7}	615

3.2. The Electrochemical Impedance Spectroscopy (EIS)

The EIS impedance data for the Bare and BZI-AA2024 samples run-in period of the 144 h of immersion test is shown in Figure Starting from one hour of immersion of the Bare-AA2024, a low impedance of about 3 ohms.cm^2 was observed at high frequencies between 10^3 and 10^5 Hz. This is attributed to surface interface and solution resistance. Fur-

thermore, it slightly decreased to about 2.6 ohms.cm^2 after 144 h immersion at a low frequency from 0.1 to 0.01 Hz; the impedance generally decreased from the first hour until 144 h.

The impedance data for the BZI-AA2024 substrate, as shown in Figure 3, showed the EIS results in one hour of immersion expose nominal impedance, starting at about 8 ohms. cm^{-2} that might be attributed to surface interface solution resistance at high frequency between 10^5 to 10^3 Hz, then starting rising with slightly sloping to reach the higher magnitude in the low frequencies between 1.0 to 0.01 Hz with value about 3.3×10^5 ohms. cm^{-2}, which is higher by two orders of magnitude than the Bare-AA2024 sample. However, from 24 until 144 h, two time-constants were observed, the first time constant started from 10^5 to 10^3 Hz, and the second one began from 10 to 0.1 Hz. These two time-constants could be attributed to the integration of BZI film and the aluminium oxide film on the substrate.

After 24 h of the immersion period, it continues to behave similarly as a coated sample, which shows a degree of protection. At low frequencies from 0.1 to 0.01 Hz, the impedance decreased dramatically from the first hour to 144 h to reach about 2.0×10^5 ohms. cm^{-2}. This suggests the possibility of creating a film of benzimidazole on the substrate to save the AA2024-T3 alloy from direct corrosion. Furthermore, the phase angle θ plot for BZI -AA2024 showed one big time-constant in the first immersion hour, between 10^3 to 0.1 Hz; these are attributed to the created BZI film layer, which came from the sample treatment process. After 24 h until 144 h, it showed two time-constant, which shifted from around 100 Hz to around 10 Hz. These two time-constants could be attributed to the integration of BZI film and the aluminium oxide film on the substrate. While the bare Aa2024 kept on a time-constant from first until 144 h.

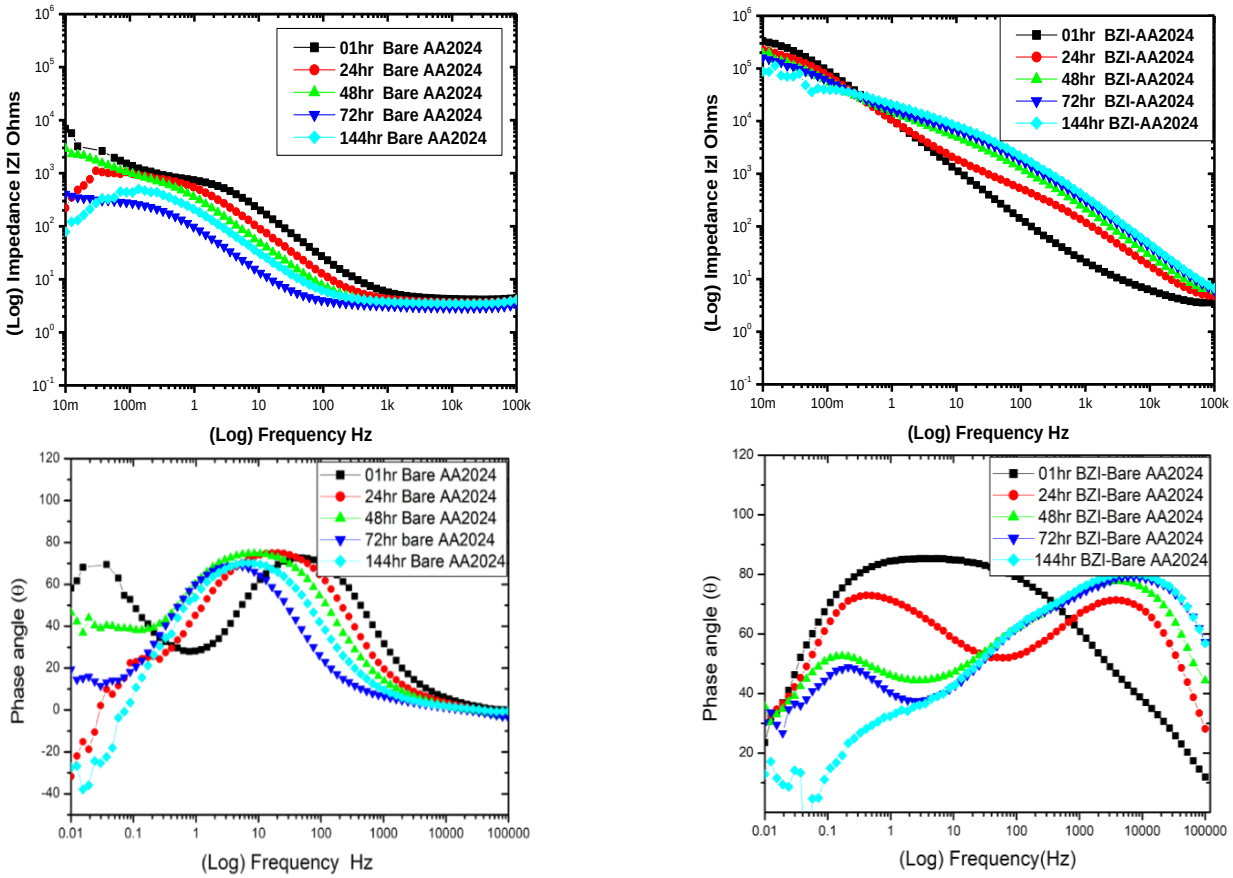

Figure 3. Impedance behaviour and Phase angle response of Bare and BZI-coated-AA2024 in 3.5% NaCl solution.

3.3. Chemical Composition and Adsorption Confirmation

3.3.1. Energy-Dispersive X-ray Spectroscopy (EDX)

The trace of the benzimidazole after 144 h of testing in 3.5% NaCl on the surface of AA 2024-T3 substrate was checked by using the EDX technique. by using EDX analysis, as shown in Figure 4a,b, the spectrum showed a minimal trace of nitrogen which reflects the presences of an azole group on the surface. By zooming-in, the spectrum from 0.1 to 2.0 KeV shows the peak shoulder confirmed the nitrogen at about 0.4 KeV by element weight percentage of 1.0~1.1 wt.% [18].

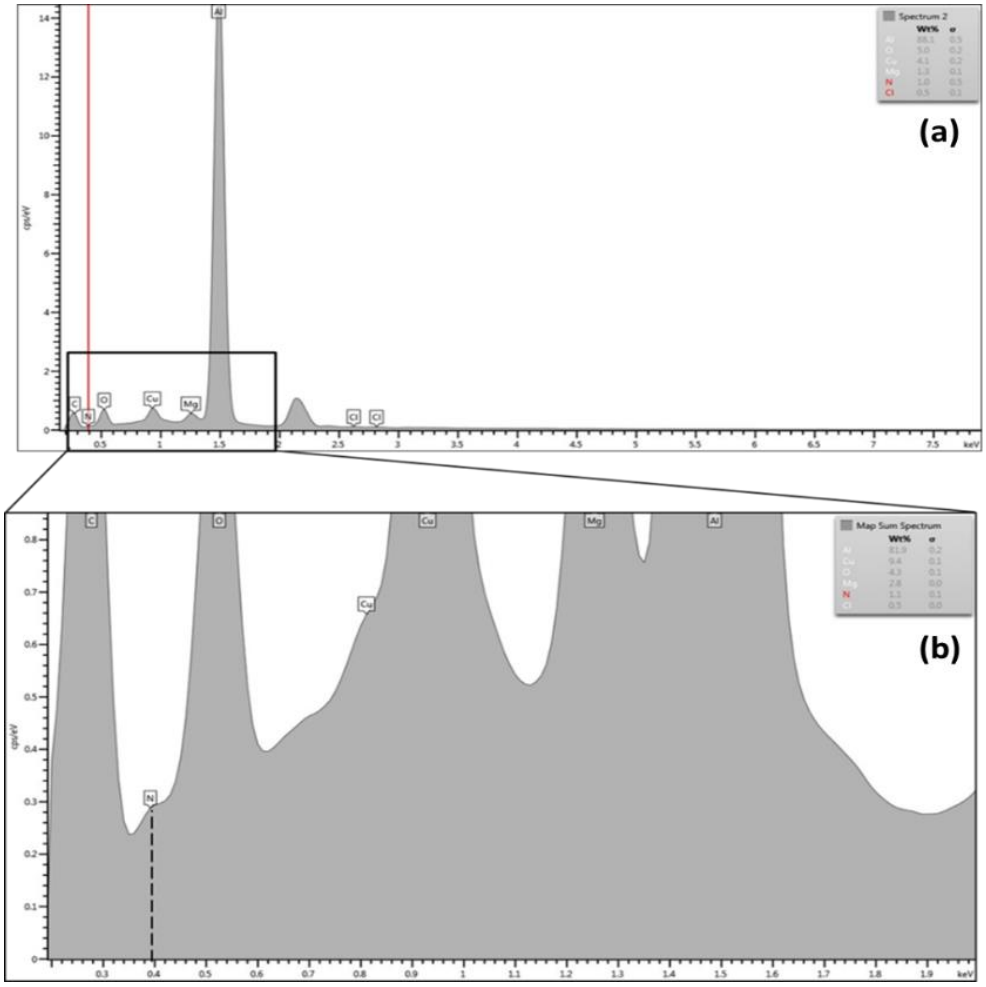

Figure 4. (**a**) EDX spectrum, (**b**) zoomed spectrum showing the trace of nitrogen adsorption on the AA2024-T3 after 144 h of immersion.

3.3.2. ATR-FTIR Data Analysis of Chemical Confirmation

FTIR data confirm the presence of Benzimidazole (BZI) film adsorption on the surface of AA2024 substrate before and after immersion. The Benzimidazole FTIR is carried out as a control and is presented in Figure Numerous vibration modes are characteristic of the BZI molecule. Also, these peaks and stretches can be observed and remain on the BZI-AA2024 sample after treatment. The imine C=N stretching is present at 1588 cm^{-1}, and additional carbon double bond C=C stretching peaks are confirmed at 1478 cm^{-1}, 1459 cm^{-1} and 1410 cm^{-1}, respectively.

Likewise, the fingerprint of the aromatic amine stretching C-N can be detected at 1365, 1348 and 1302 $cm^{-1,}$ respectively, confirm the benzimidazole presence on the substrate. These stretching peaks keep their position even after long immersion, which might

be attributed to the BZI reacting with a metallic surface. A weak group of peaks characterise the C-H out-of-plane bending at 958,885,769 and 750 cm^{-1} [19,20].

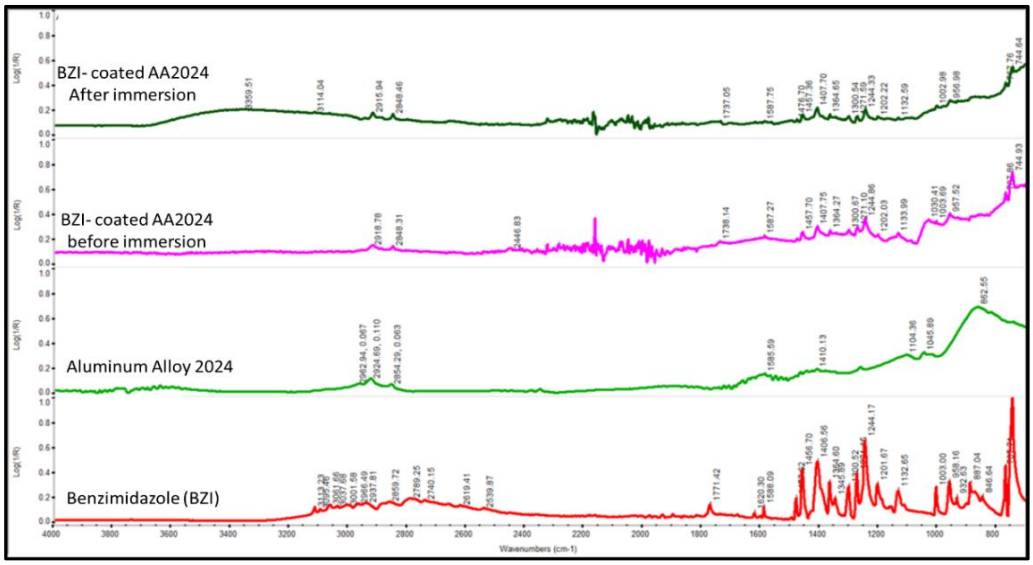

Figure 5. Contact mode ATR spectrum for BZI-AA2024 sample before and after immersion in 3.5% NaCl solution.

Although there was a trace of adsorption of benzimidazole after 144hr of immersion, hydration taking place due to diffusion action, and as a result of this OH- stretching appears at low intensity in the region between 3000 and 3400 cm^{-1} attributed to aluminium hydroxide Al-OH film and the remained propagated H_2O in the interfacial and oxidised layer [19,21,22].

3.4. Scanning Electron Microscopy Images (SEM)

Figure 6 shows the surface morphology of both samples, BZI-AA2024 and bare alloy AAIt is clear that the bare sample is attacked by pitting corrosion after long immersion of 144 h, as showed in Figure 6a. On the other hand, the BZI-AA2024 coated sample showed excellent resistance to corrosion under similar circumstances, in Figure 6b. Furthermore, the measurements showed that the ZBI- was more stable in the salty water 3.5% NaCl, which may attributed prevent the diffusion in the coating system, in line with the benzimidazole self-healing inhibition properties.

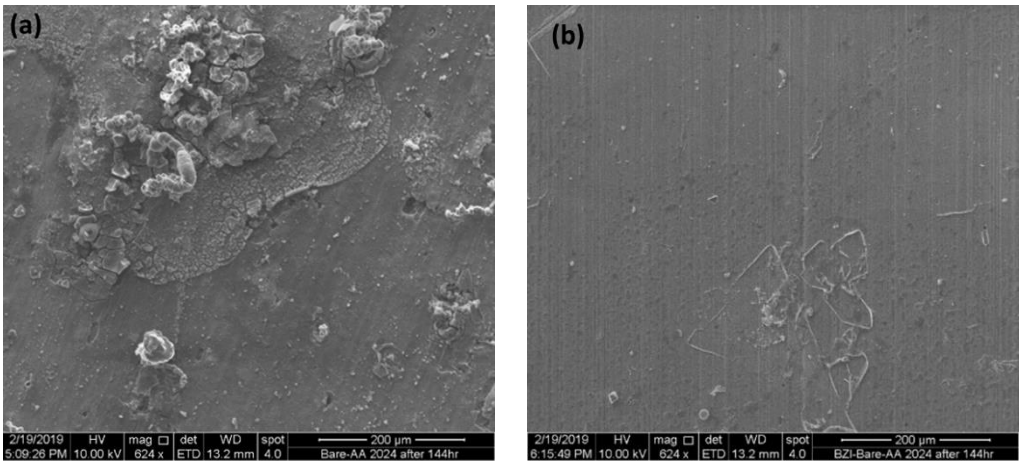

Figure 6. Shows the bare and BZI-AA2024 sample after immersed in 3.5% NaCl solution with (**a**) SEM image with no creation of pitting corrosion.

4. Conclusions

Electrochemical testing techniques Evaluating the spraying of the benzimidazole solution on aluminium alloys 2024-T3 revealed excellent corrosion protection when combined with the nontreated sample, which can provide protection over one week without any failure or pitting sign on the surface in an aggressive medium of 3.5 % NaCl. Furthermore, applying benzimidazole as a film-forming inhibitor to the surface provides simulated active protection due to the high electronegativity of the active azole group. Also, it gains the highest impedance when compared to the noncoated AA 2024-TAs it is cost-effective, the BZI could be used instead of the traditional ways of storing aluminium alloys for short terms.

Funding: This research received no external funding.

Institutional Review Board Statement: Not applicable.

Informed Consent Statement: Not applicable.

Data Availability Statement: The data are not publicly available; the files are stored on corresponding instruments and personal computers.

Acknowledgments: The authors would like to acknowledge the Libyan scholarship programme and Sheffield Hallam University for facilitating support.

Conflicts of Interest: The authors declare no conflict of interest.

References

1. Tiringer, U.; Kovač, J.; Milošev, I. Effects of mechanical and chemical pre-treatments on the morphology and composition of surfaces of aluminium alloys 7075-T6 and 2024-T. *Corros. Sci.* **2017**, *119*, 46–59, doi:10.1016/j.corsci.2017.02.018.
2. Boag, A.; Hughes, A.E.; Glenn, A.M.; Muster, T.H.; McCulloch, D. Corrosion of AA2024-T3 Part I: Localised corrosion of isolated IM particles. *Corros. Sci.* **2011**, *53*, 17–26.
3. Vargel, C. *Corrosion of Aluminium*; 1st ed.; Elsevier Science B.V: Oxford, UK, 2004.
4. Mussa, M. Development of Hybrid Sol-Gel Coatings on AA2024-T3 with Environmentally Benign Corrosion Inhibitors.Thesis, Sheffield Hallam University, 2020.
5. Polmear, I.; StJohn, D.; Nie, J.-F.; Qian, M. Physical metallurgy of aluminium alloys. In *Light Alloys*; Butterworth-Heinemann, Elsevier Ltd.: Oxford, UK, 2017; pp. 31–107, ISBN 9780080994314.
6. Wang, S.C.; Starink, M.J. Precipitates and intermetallic phases in precipitation hardening Al–Cu–Mg–(Li) based alloys. *Int. Mater. Rev.* **2005**, *50*, 193–215.
7. Buchheit, R.G.; Grant, R.P.; Hiava, P.F.; Mckenzie, B.; Zender, G. Local Dissolution Phenomena Associated with S Phase (AI2CuMg) Particles in Aluminum Alloy 2024-T*J. Electrochem. Soc.* **1997**, *144*, 2621.
8. Okafor, A.C.; Nnadili, C. *Journal of Failure Analysis and Prevention* **2012**, 670–682.
9. Mussa, M.H.; Rahaq, Y.; Takita, S.; Farmilo, N. Study the Enhancement on Corrosion Protection by Adding PFDTES to Hybrid Sol-Gel on AA2024-T3 Alloy in 3.5% NaCl Solutions. *Albahit J. Appl. Sci.* **2021**, *2*, 61–68.
10. Andreev, N.N.; Kuznetsov, Y.I. Volatile inhibitors of metal corrosion. I. vaporization. *Int. J. Corros. Scale Inhib* **2012**, 16–25.
11. Bastidas, D.M.; Cano, E.; Mora, E.M. Volatile corrosion inhibitors: A review. *Anti-Corrosion Methods Mater.* **2005**, *52*, 71–77.
12. Wright, J.B. The Chemistry of the Benzimidazoles. *Chem. Rev.* **1951**, *48*, 397–541.
13. Obot, I.B.; Madhankumar, A.; Umoren, S.A.; Gasem, Z.M. Surface protection of mild steel using benzimidazole derivatives: Experimental and theoretical approach. *J. Adhes. Sci. Technol.* **2015**, *29*, 2130–2152.
14. Gutiérrez, E.; Rodríguez, J.A.; Cruz-Borbolla, J.; Alvarado-Rodríguez, J.G.; Thangarasu, P. Development of a predictive model for corrosion inhibition of carbon steel by imidazole and benzimidazole derivatives. *Corros. Sci.* **2016**, *108*, 23–35.
15. Gupta, P.K. Herbicides and fungicides. In *Biomarkers in Toxicology*; Elsevier Inc.: Amsterdam, The Netherlands, 2014; pp. 409–431, ISBN 9780124046306.
16. ASTM International ASTM code B209—14 Standard Specification for Aluminum and Aluminum-Alloy Sheet and Plate. **2016**, *25*, 16.
17. Tait, W.S. *Electrochemical Impedance Spectroscopy Fundamentals, an Introduction to Electrochemical Corrosion Testing for Practicing Engineers and Scientists*; Tait, W.S., Ed.; PairODocs Publications: Racine, WI, USA, 1994; ISBN 13-978-0966020700.
18. Fateh, A.; Aliofkhazraei, M.; Rezvanian, A.R. Review of corrosive environments for copper and its corrosion inhibitors. *Arab. J. Chem.* **2017**, 1–63.
19. Mohan, S.; Sundaraganesan, N.; Mink, J. FTIR and Raman studies on benzimidazole. *Spectrochim. Acta Part A Mol. Spectrosc.* **1991**, *47*, 1111–1115.
20. Thermo scientific Knowledge base infrared spectral interpretetion. 2009, 1–77.

21. Usoltseva, N.V.; Korobochkin, V.V.; Balmashnov, M.A.; Dolinina, A.S. Solution Transformation of the Products of AC Electrochemical Metal Oxidation. *Procedia Chem.* **2015**, *15*, 84–89.
22. Loehle, S. Understanding of Adsorption Mechanisms and Tribological Behaviors of C18 Fatty Acids on Iron-Based Surfaces: A Molecular Simulation approach. Ph.D. Thesis. Université de Lyon, Lyon, France, 2014.